Estimation of Tracer kinetic Parameters from undersampled DCE-MRI data using a Non-Linear Tracer Kinetic model

Shwetha S

Sri Sivasubramaniya Nadar College of Engineering, Rajiv Gandhi Salai (OMR), Kalavakkam, Tamil Nadu, India. PIN: 603110

Dr. Phaneendra Kumar Yalavarthy

Associate Professor, Department of Computational and Data Sciences (CDS), Indian Institute of Science, Bangalore, India. PIN: 560012

Table of Contents

Estimation of Tracer kinetic Parameters from undersampled DCE-MRI data using a Non-Linear Tracer Kinetic model

Shwetha S

Sri Sivasubramaniya Nadar College of Engineering, Rajiv Gandhi Salai (OMR), Kalavakkam, Tamil Nadu, India. PIN: 603 110

Dr. Phaneendra Kumar Yalavarthy

Associate Professor, Department of Computational and Data Sciences (CDS), Indian Institute of Science, Bangalore, India. PIN: 560012.

Abstract

Dynamic contrast-enhanced magnetic resonance imaging (DCE-MRI) is the acquisition of sequential images of the tissue of interest after intravenous administration of a contrast agent. It has various clinical applications, such as distinguishing benign & malignant tissues and detection of areas of viable tumour before biopsy. DCE-MRI derived parameters like Ktrans are valuable in the evaluation of tumour response to therapy including non-cytotoxic agents that target tumour vascularity. These parameters also provide information on tissue vascularization, vascular permeability, perfusion and composition of the extracellular extravascular space (EES). The drawback of this imaging method is that it requires high temporal resolution so as to capture the changes in the concentration of the contrast agent through each voxel, which in turn reduces spatial resolution. Undersampling of MRI data through compressed sensing and parallel imaging techniques reduces the acquisition time and helps in increasing the spatial resolution. In conventional reconstruction methods, intermediate images are reconstructed from undersampled data before modelling of the Tracer kinetic (TK) Parameters. Several models such as Etofts and Patlak are utilized to model these TK parameters. Appropriate model is chosen based on prior knowledge and a data driven basis. Research by Yi Guo et al. demonstrated Direct Estimation of TK Parameter Maps from highly undersampled MRI data using the Patlak model. However, the demonstrated technique was applied only for Patlak Model which is linear in nature and as a result the optimization was straightforward. In order to accommodate various tissue structures, this method needs to be extended to higher dimensional models. This will involve solving a highly non-linear minimization problem. The purpose of this work is to estimate TK parameters directly from undersampled DCE MRI data using a higher dimensional Etofts (Extended tofts) model which has three parameters - Ktrans, Vp and Kep. It is widely used for DCE MRI and is applicable for highly perfused tissues as well as weakly vascularized tissues with a well-mixed EES. This work demonstrates the estimation of TK parameters from undersampled MRI data using Etofts model at various undersampling rates.

Keywords: DCE-MRI, Tracer Kinetic Parameters, Perfusion Imaging, Tracer Kinetic models, Tumour Response

Abbreviations

MR	Magnetic Resonance
DCE MRI	Dynamic Contrast Enhanced Magnetic Resonance Imaging
CA	Contrast Agent
ROI	Region of Interest
TK	Tracer Kinetic
TIC	Time Intensity Curve
EES	Extracellular Extravascular space
AIF	Arterial Input Function
Etofts	Extended Tofts
TV	Total Variation

1 INTRODUCTION

1.1 Background/Rationale

The cells in our body are always within 100-200 μm of blood vessels as they require oxygen and nutrition (Rakesh K. Jain, 2000). As a tumour grows, it moves farther away from these vessels while also requiring increasing amounts of oxygen, nutrients and a pathway to remove cellular waste. This is when the tumour starts to form its own vasculature in a process known as tumour angiogenesis (Fig 1). The vasculature formed by the tumour is disorganized, leaky in nature and has blind ends & bulges. As a result, it can be characterized by the leakage of a contrast agent (CA) administered to a vessel near the region of interest (ROI). Quantitative parameters that describe this perfusion and permeability are valuable when making a diagnosis on the nature of the tumour. Dynamic Contrast Enhanced Magnetic Resonance Imaging (DCE-MRI), a relatively new imaging technique, can be employed to extract this information.

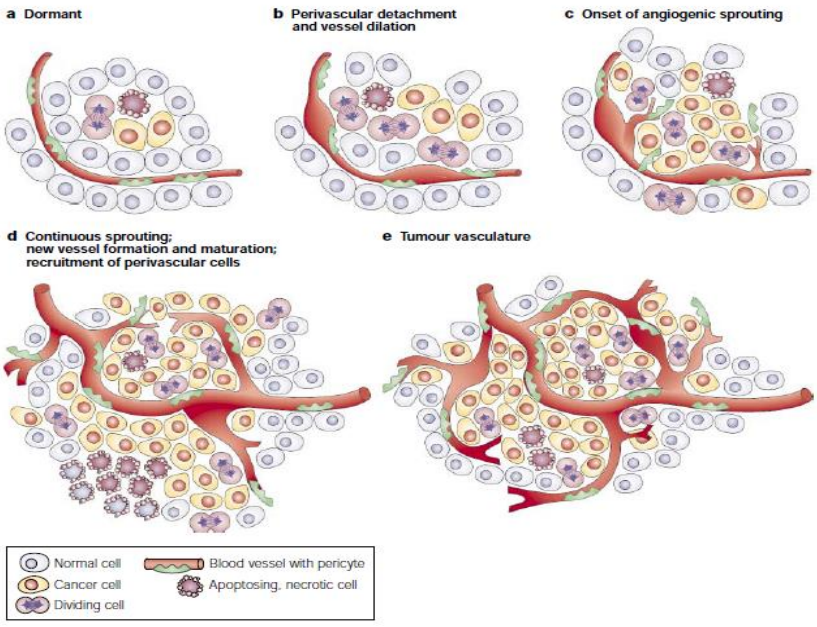

Fig 1 Depiction of Tumour Angiogenesis adapted from Bergers, et al, 2003

DCE-MRI, however, requires high temporal resolution to capture the changes in CA concentration in the ROI, which in turn reduces the spatial resolution. This can be addressed using compressive sensing and parallel imaging techniques, which increase the spatial resolution by recovering high quality anatomical images from undersampled k-t space. Earlier studies focused on the reconstruction of MR image time series from this k-t space before construction of the TK parameter maps. This approach is commonly known as indirect technique and it does not lead to good quality TK maps at high acceleration rates. Contrary to indirect techniques, direct techniques estimate TK parameters from undersampled k-t space data without reconstructing anatomical images. Research by Guo, et al, 2016 demonstrated the estimation of parameter maps directly from the undersampled k-t space at high acceleration rates for a linear tracer kinetic model - Patlak model.

The objective of this work is to extend the concept of Direct Reconstruction to a non-linear tracer kinetic model - Extended Tofts Model.

1.2 DCE-MRI

MRI is a well-established non-ionizing imaging modality, but MR imaging with Nyquist sampling is unable to provide high spatial resolution without a significant increase in acquisition time. In order to achieve greater imaging speeds, parallel imaging and compressive sensing techniques are employed to subsample the k space. Parallel Imaging methods such as SENSE (Peter Boesiger, 1999) and GRAPPA (Griswold, et al, 2002) involve the usage of multiple coils to image the ROI. The inherent sparsity of MR images in either the image domain or in some other transform domain can be exploited to subsample the k space, provided that the k space is sampled randomly and aliasing artifacts are incoherent in the above-mentioned domain in which the MR image is sparse. This approach is formally known as compressed sensing (Lustig, et al, 2007). These methods are employed together to accelerate the process of image acquisition without significant loss of image quality.

These techniques are also employed to DCE-MRI where high spatiotemporal resolution is required. Dynamic contrast-enhanced magnetic resonance imaging (DCE-MRI) is the acquisition of T1-weighted sequential images of the tissue of interest after intravenous administration of a CA (tracer). The CA is usually a gadolinium compound which reduces the relaxation time of water protons. Therefore, the images acquired after the administration of CA show signal enhancement. There exists a non-linear relationship between the concentration of the CA and the signal acquired for various pulse techniques. Due to the presence of CA in the ROI, the T1 map acquired before administration (T10) is reduced to a value T1. This relation can be expressed as shown below –

$$\frac{1}{T1(x,y,z,t)} = \frac{1}{T10(x,y,z)} + Rcs * C\left(x,y,z,t\right) \tag{1}$$

where *Rcs* is the relaxivity of the CA administered and *C(x,y,z,t)* is the concentration of CA in the ROI.

The dynamic DCE Image Series obtained by employing the Spoiled Gradient Recalled Acquisition in Steady State (SPGR) pulse technique is given by eqn (2).

$$s(x,y,z,t) = \frac{M_0(x,y,z)sin\alpha\left(1-e^{(-TR/T_1(x,y,z,t))}\right)}{\left(1-cos\alpha.e^{(-TR/T_1(x,y,z,t))}\right)} + \left[s\left(x,y,z,0\right) - \frac{M_0(x,y,z)sin\alpha\left(1-e^{(-TR/T_{10}(x,y,z))}\right)}{\left(1-cos\alpha.e^{(-TR/T_{10}(x,y,z))}\right)}\right] \tag{2}$$

Here, $s(x,y,z,t,)$ is the time series of the DCE-MRI images obtained, TR is the temporal resolution and α is the flip angle. $s(x,y,z,0)$ is the pre-contrast frame in the image time series and is fully sampled, $T_{10}(x,y,z)$ is the pre-contrast T1 map and $M_0(x,y,z)$ is the longitudinal magnetization estimated from the T1- mapping sequence DESPOT1. In eqn (2) the term in parentheses is included to account for the difference between the pre-contrast signal and the predicted pre-contrast signal based on baseline T10 and M0 maps (Guo, et al, 2016).

By combining equations (1) and (2), the concentration of the CA in the ROI can be obtained for each voxel. In other words, the acquired signal is used to generate a Time Intensity Curve (TIC) for each voxel which mirrors the tissue's response to the entry and exit of the CA. The TIC in itself carries valuable information that can be used for diagnosis without further analysis. This semi-quantitative analysis yields metrics such as initial area under the curve, time to peak and slope of the wash in/out curve. One of the disadvantages of this approach is that the metrics obtained are not direct measures of the underlying physiology in the ROI.

1.2.1 Tracer Kinetic Models

In order to extract more information about the ROI such as the volume fractions of the subspaces and the transfer constants, model-based analysis is required. The transfer of CA between the vasculature and the Extracellular Extravascular Space (EES) can be characterized by Tracer Kinetic / Pharmacokinetic models. For DCE MRI, the terms Tracer Kinetic (TK) model and Pharmacokinetic model are used interchangeably. Different models have different assumptions about the structure of the tissue and quantize parameters that ultimately describe the permeability and perfusion of the tissue of interest. Model selection is mainly based on prior knowledge and a data driven basis.

Model based TK parameter analysis is based on the concept of compartments. A compartment is simply a well-mixed region with a constant volume in which the concentration of the CA is uniform. Mathematically 2*n parameters can be fitted for an n-compartment model. While models that have a greater number of TK parameters can describe the ROI's permeability and perfusion better, they are also prone to higher errors during non-linear fitting.

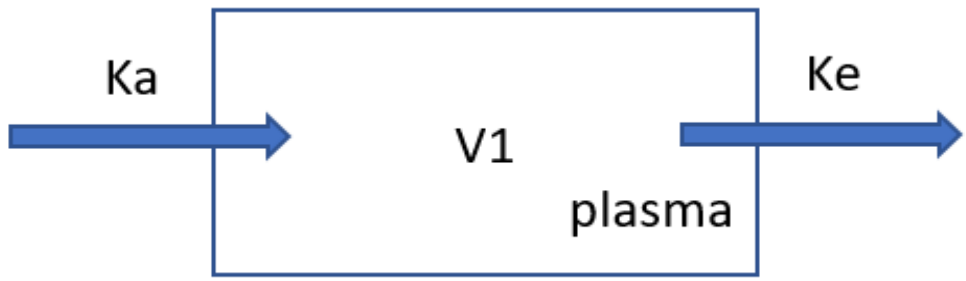

Fig 2 One Compartment model assumes that the body is a single compartment with a fixed volume V1. Rate constants Ka and Ke describe the entry and exit of the contrast agent.

The single compartment model shown in Fig (2) is the least complicated and describes the body as a single compartment with a fixed volume V1 and with two rate constants Ka and Ke which quantize the entry and the exit of the CA. Here, it is assumed that the CA spreads uniformly all over the body. However, this model is not realistic as the CA diffuses into different tissues at different rates. The tracer kinetics of the CA are better described by a two-compartment model.

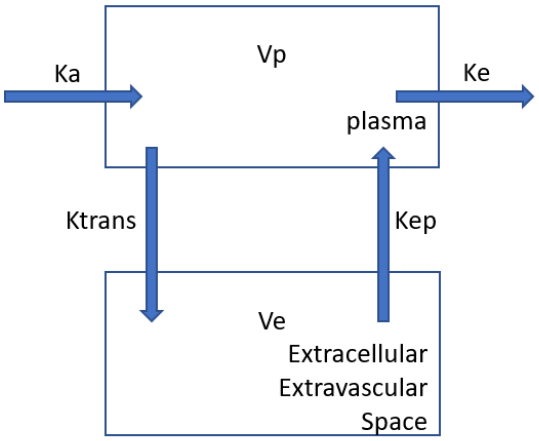

Fig 3 Two Compartment Model.

The extracellular intravascular space (plasma) is considered as the central component while the extracellular extravascular space (EES) is considered as the peripheral component. Rate constants Ka and Ke describe the entry and exit of the CA while Ktrans and Kep describe the movement of CA from plasma to EES and EES to plasma respectively.

The two-compartment model shown in Fig (3) is more realistic. The rate constants Ka characterizes the entry of CA into the blood plasma after intravenous administration and the rate constant Ke characterizes the exit of the CA from the blood plasma. Ktrans and Kep are the rate constants that quantize the movement of CA from plasma to EES and EES to plasma respectively. This model describes the vasculature as the central component through which the CA arrives into the ROI and diffuses into the peripheral compartment, the EES. Models based on the Two Compartmental Model include two chamber exchange model (2cxm), Patlak model and the Extended tofts model (Etofts). The parameters used to characterize the permeability and perfusion of a ROI were generalized in a review (Tofts, et al, 1999). Some of the important parameters are shown in Table 1.

Table 1 Tracer Kinetic Parameters

Quantity	Definition	Unit
Ktrans	Volume transfer constant for plasma to EES exchange	min^{-1}
Kep	Volume transfer constant for EES to plasma exchange	min^{-1}
Vp	Fractional plasma volume	None
Ve	Fractional EES volume	None
Fp	Arterial Plasma Flow	ml g^{-1} min^{-1}
PS	Permeability Surface Area Product	ml min^{-1} g^{-1}
AIF	Arterial Input Function	mmol/L

In order to derive quantitative TK parameters from the TIC, the arterial input function (AIF) is required. The AIF gives an estimate of the tracer concentration as a function of time in the feeding artery. The concentration of the CA $C(x,y,z,t)$ in the ROI and the AIF are related by an unknown tissue characteristic impulse response $I(t)$. The following equation represents this relation neglecting the spatial coordinates (x,y,z).

$$C(t) = I(t) \otimes AIF(t) \quad (3)$$

Obtaining the AIF is paramount for almost all quantitative models and is one of the challenging aspects of employing DCE MRI. It can be acquired by drawing blood using an arterial catheter from the patient periodically during the scan. Though this method provides an accurate estimation of the AIF, it is invasive and presents ambiguity about the time at which each sample is drawn. Another method is to assume that the AIF is the same for all patients and use a predetermined value for the calculation of TK parameter maps. Though this takes away the need to acquire AIF during the scan, it can cause a significant change in the values of the TK parameters because realistically the AIF varies from patient to patient. The third method is to obtain the AIF from the DCE-MRI datasets themselves. For this, techniques that convert blood signal intensity into CA concentration in blood are employed. This method requires a large vessel to be in the field of view which may not be the case always. Apart from these methods, reference region models that do not require AIF are also under research. Recently a study (Guo, et al, 2017) modelled AIF as one of the parameters to be fitted along with the TK Parameters.

1.2.2 Patlak model

The Patlak model describes tissues that are highly perfused. It characterizes the ROI as two TK parameters, Ktrans and Vp. The concentration of the CA in the ROI is described by eqn (4). As this model is linear, Ktrans and Vp can be found by simply taking the pseudoinverse. It can be considered as a simplification of the Etofts model where the CA influx from the EES to plasma is assumed to be negligible. The relationship between the TK parameters and CA concentration is shown below. For brevity, in the following equation the spatial coordinates *(x,y,z)* are neglected and the relation is expressed with respect to time.

$$C(t) = Vp \,.\, AIF(t) + Ktrans \int_0^t AIF(\tau)\, d\tau \quad (4)$$

1.2.3 Etofts model

The Extended Tofts (Etofts) Model describe tissues that are either highly perfused or weakly vascularized with a well-mixed EES. It assumes bidirectional transport between the two compartments. It characterizes the microvasculature using three TK parameters : Ktrans, Kep and Vp. One of the drawbacks of the Etofts model is that it assumes Fp to be infinite (highly perfused). As a result, if it is applied to tissues with low to moderate Fp it severely underestimates the value of Vp. Despite this drawback, Etofts model is widely used because it is able to realize the TK parameters even at low temporal resolution. The relationship between the TK parameters and CA concentration with respect to time is shown in eqn (5).

$$C(t) = Vp \,.\, AIF(t) + Ktrans \int_0^t AIF(\tau)\, exp(-Kep(t-\tau))\, d\tau \quad (5)$$

2 LITERATURE REVIEW

2.1 Conventional reconstruction of parameter maps from under sampled data

The conventional reconstruction of TK parameter maps from MR Images acquired at high acceleration rates takes place as shown in Fig (4). The undersampled k-t space data acquired at various time instances is converted into image series by solving the minimization problem in eqn (6). This image series is then used to obtain the TIC for each voxel which is then fitted for the required model.

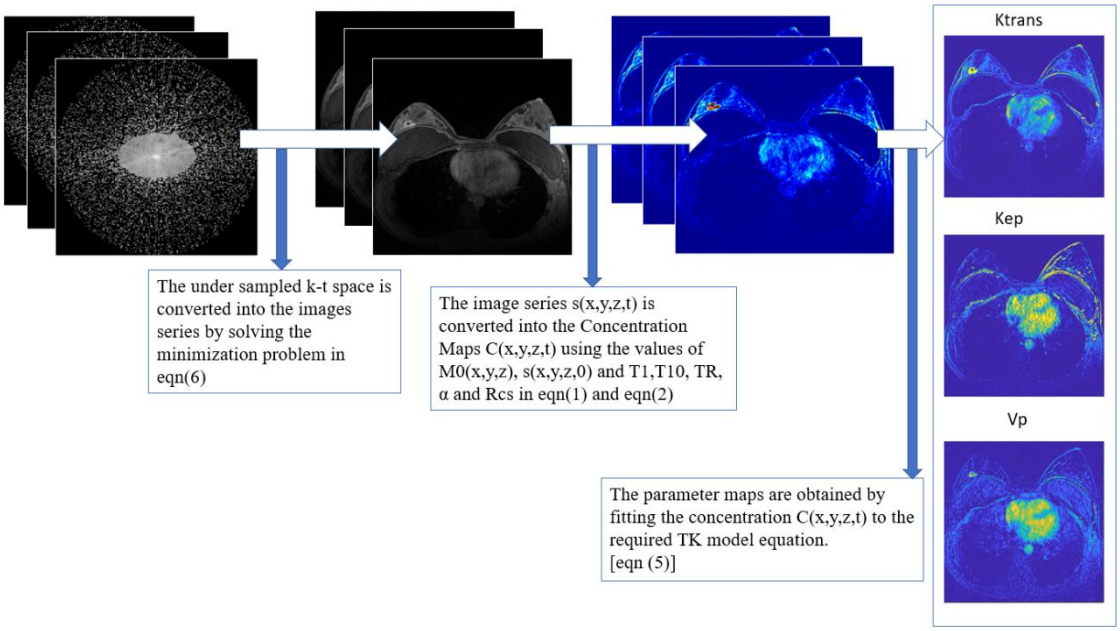

Fig 4 Indirect Reconstruction of Ktrans, Kep and Vp from the undersampled k-t space

Methods developed by researchers employ the following minimization problem that include constraints that force the solution to be sparse in transform domains. These 'indirect methods' can give acceptable results for acceleration rates of up to 36x. In the below equation, L1 norm is applied to enforce sparsity in wavelet (ψ) and temporal finite differences (V) domains.

$$s(r,t)=\underset{s(r,t)}{argmin} \parallel S_F\left(k,t,c\right) - F_u C\left(r,c\right) s\left(r,t\right) \parallel_2^2 + \lambda_1 \parallel Vs\left(r,t\right) \parallel_1 + \lambda_2 \parallel \psi s\left(r,t\right) \parallel_1 \qquad (6)$$

where r is a vector that encapsulates the spatial coordinates *(x, y, z)*, *k* is a vector that represents the k space coordinates *(kx, ky, kz)*, *t* is the time dimension and *c* is the coil dimension. Here, *s(r,t)* is the reconstructed image series, S_F *(k,t,c)* is the undersampled k-t space obtained, F_u is the undersampling Fourier Transform and *C(r,c)* is the coil sensitivities. *V* is the temporal finite differences transform and ψ is the spatial wavelet transform. The same notation is followed through the rest of this work.

2.2 Direct Reconstruction of parameter maps from under sampled data

A model-based approach to directly estimate the parameter maps from the undersampled k-t space was initially shown by Felsted, et al, 2009. They employed a modified gradient descent scheme to minimize the difference between the undersampled k-t space and the k-t space from the estimated parameter maps. They demonstrated reasonable accuracy of parameter maps for acceleration rate R=4. Similarly, Dikaios, et al, 2014 suggested a Bayesian inference framework to estimate TK parameters directly at high temporal resolution. They demonstrated better correspondence of directly derived TK parameters to the ground truth TK parameters of phantom when compared to indirect methods for the Etofts model. They were able to achieve 8x acceleration in phantom data and in vivo prostate data. Guo, et al, 2016 were able to demonstrate upto 100x acceleration and also provided a parameter free reconstruction of TK parameter maps from undersampled data using Patlak model. However, pre-contrast T1 and M0 maps need to be known and prior knowledge of AIF is required. Their work also did not include non-linear higher order models such as Etofts model and Two Chamber Exchange Model (2cxm).

3 METHODS

3.1 Concepts

3.1.1 Formulation of the minimization problem

We estimate the TK parameters from the undersampled (k-t) space by solving the minimization problem in eqn (7). A forward model that converts the TK parameters to the undersampled k-t space is shown in Fig (5). The cost function *y(Ktrans, Kep, Vp)* in eqn (8) includes this forward model and computes the difference between the undersampled k-t space acquired by the scanner and the undersampled k-t space calculated by the forward model.

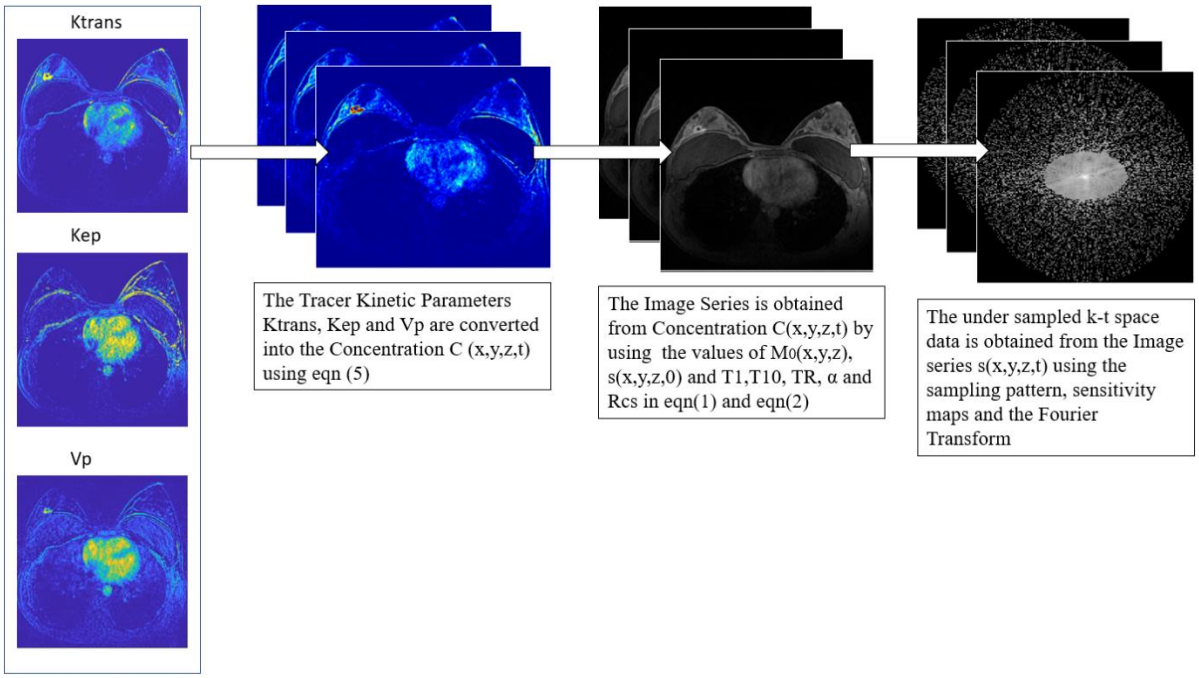

Fig 5 Forward model that converts the TK parameters Ktrans, Kep and Vp into the undersampled k-t space.

$$\textit{Minimization Problem}: \quad (Ktrans(r), Kep(r), Vp(r)) = \underset{Ktrans(\mathrm{r}),\, Kep(\mathrm{r}),\, Vp(\mathrm{r})}{argmin} \| S_F(k,t,c) - f(Ktrans(\mathrm{r}),\ Kep(\mathrm{r}),\ Vp(\mathrm{r}) \|_2^2 \qquad (7)$$

Here $f(Ktrans(r), Kep(r), Vp(r))$ is a function that converts the TK parameters into the undersampled k-t space.

$$\textit{Cost function}: \quad y(Ktrans(r), Kep(r), Vp(r)) = \| S_F(k,t,c) - f(Ktrans(r), Kep(r), Vp(r)) \|^2_2 \qquad (8)$$

This non-linear minimization problem in eqn (7) is solved by using limited-memory Broyden-Fletcher-Goldfarb-Shannon (l-BFGS) method. The library minFunc (M. Schmidt, 2005) was used in MATLAB

(MATLAB, 2018) to employ this method. The TK parameters can be vectorized to optimize all the TK parameters at the same time as shown in eqn (9) or they can be optimized alternately as shown in eqn (10).

Algorithm for optimization of all TK parameters at the same time

$$
\begin{aligned}
&j = 0 \\
&A = [vec(Ktrans(r));\ vec(Kep(r));\ \ vec(Vp(r))] \\
&while(condition) \\
&\{ \\
&A^{(j+1)} = \underset{A^{(j)}}{argmin} \ \left\| S_F(k,t,c) - f(A^{(j)}) \right\|_2^2 \\
&j = j + 1 \\
&\}
\end{aligned}
\tag{9}
$$

Algorithm for Optimization of TK parameters one at a time:

$$
\begin{aligned}
&k = 0 \\
&while(condition) \\
&\{ \\
&Ktrans(r)^{(k+1)} = \underset{Ktrans\ (r)^{(k)}}{argmin} \left\| S_F(k,t,c) - f(Ktrans(r)^{(k)},\ Kep(r)^{(k)}, Vp(r)^{(k)}) \right\|_2^2 \\
&Kep(r)^{(k+1)} = \underset{Kep(r)^{(k)}}{argmin} \left\| S_F(k,t,c) - f(Ktrans(r)^{(k+1)},\ Kep(r)^{(k)}, Vp(r)^{(k)}) \right\|_2^2 \\
&Vp(r)^{(k+1)} = \underset{Vp\ (r)^{(k)}}{argmin} \ \left\| S_F(k,t,c) - f(Ktrans(r)^{(k+1)},\ Kep(r)^{(k+1)} Vp(r)^{(k)}) \right\|_2^2 \\
&k = k + 1 \\
&\}
\end{aligned}
\tag{10}
$$

The gradient of the cost function is found with respect to the three TK parameters of Etofts model by applying the chain rule. For simplicity, in the following equations the coordinates *r*, *k* and *c* are neglected while *t* is retained. In eqn (15), R1(t) is the relaxation rate and it is the reciprocal of T1(t).

$$
\frac{\partial y(Ktrans,Kep,Vp)}{\partial Ktrans} = \frac{\partial y(Ktrans,Kep,Vp)}{\partial s(t)} \cdot \frac{\partial s(t)}{\partial C(t)} \cdot \frac{\partial C(t)}{\partial Ktrans} \tag{11}
$$

$$
\frac{\partial y(Ktrans,Kep,Vp)}{\partial Kep} = \frac{\partial y(Ktrans,Kep,Vp)}{\partial s(t)} \cdot \frac{\partial s(t)}{\partial C(t)} \cdot \frac{\partial C(t)}{\partial Kep} \tag{12}
$$

$$
\frac{\partial y(Ktrans,Kep,Vp)}{\partial Vp} = \frac{\partial y(Ktrans,Kep,Vp)}{\partial s(t)} \cdot \frac{\partial s(t)}{\partial C(t)} \cdot \frac{\partial C(t)}{\partial Vp} \tag{13}
$$

$$
\frac{\partial y(Ktrans,Kep,Vp)}{\partial s(t)} = C^{H} F_u{}^{H} [\, k_u(t) - f(Ktrans, Kep, Vp) \,] \tag{14}
$$

$$\frac{\partial s(t)}{\partial C(t)} = Rcs\,.M0\,.sin\alpha\,.\frac{TRe^{-TR.R1(t)}\left(1-e^{-TR.R1(t)}cos\alpha\right)-\left(1-e^{-TR.R1(t)}\right).TRe^{-TR.R1(t)}cos\alpha}{\left(1-e^{-TR.R1(t)}cos\alpha\right)^2} \tag{15}$$

$$\frac{\partial C(t)}{\partial Ktrans} = \int_0^t [\,AIF\,(\tau) - exp\,(Kep\,(t-\tau)\,)\,]\;d\tau \tag{16}$$

$$\frac{\partial C(t)}{\partial Kep} = -\,(t-\tau)\;.\,Ktrans\int_0^t [\,AIF\,(\tau) - exp\,(Kep\,(t-\tau)\,)\,]\;d\tau \tag{17}$$

$$\frac{\partial C(t)}{\partial Vp} = AIF\,(t\,) \tag{18}$$

3.1.2 RMSE

The figure of merit used in this work is the root mean square error. The Ktrans map obtained from the fully sampled k-t space is compared with the Ktrans map obtained from the undersampled k-t space for each pixel in the tumour region.

$$RMSE = \sqrt{\sum_{i=1}^{n\times\ m}\frac{(Ktrans_{under\ sampled}-Ktrans_{fully\ sampled})^2}{n\times\ m}} \tag{19}$$

where *n* is the number of rows and *m* is the number of columns in the image of the tumour region.

3.2 Dataset

Two Datasets were used to validate the method proposed in this work. The first dataset was made available by Guo, et al, 2016. The second dataset was made available by Guo, et al, 2017. Both the datasets have spatial dimension of 256 x 150 and consists of 50-time frames obtained using eight receiver coils. They also had the following parameters, FOV: 22 x 22 x 4.2 cm3, spatial resolution: 0.9 x 1.3 x 7.0 mm3, Temporal Resolution: 5 seconds, Flip angle: 15 degrees, Echo time (TE): 1.3ms and TR: 6ms. DESPOT1 was performed before DCE MRI and three images with flip angles of 2° , 5° and 10° were obtained to estimate pre-contrast T1 and M0 maps. For DCE MRI, the CA, gadobenate dimeglumine (MultiHance Bracco Diagnostics Inc., Princeton, NJ) which has relaxivity Rcs=4.39 s-1 mM-1 at 37°C at 3T, was administered with a dose of 0.05 mMol/kg. A 20 mL saline flush was administered intravenously in the left arm after administration of CA. Both of these datasets were under sampled retrospectively using Golden Angle Radial undersampling scheme with acceleration rate R ranging from 10x to 100x.

4 RESULTS

The method proposed in this work was implemented on 2 datasets using the algorithms mentioned in eqn (9) and eqn (10). In the experiments, at the most 5o iterations were required to reach convergence. The time taken to process one slice with 256 x 150 pixels was approximately 30 mins. The experiments were performed on a Linux workstation with 64GB RAM using MATLAB R2018b (MATLAB, 2018). Fig (6) and Fig (7) depict the Ktrans obtained for various undersampling rates by optimizing all the TK parameters at once for dataset 1 and dataset 2 respectively. RMSE values with respect to the ground truth value i.e., the Ktrans map in the tumour region obtained from the fully sampled k-t space data, is given in the boxes below.

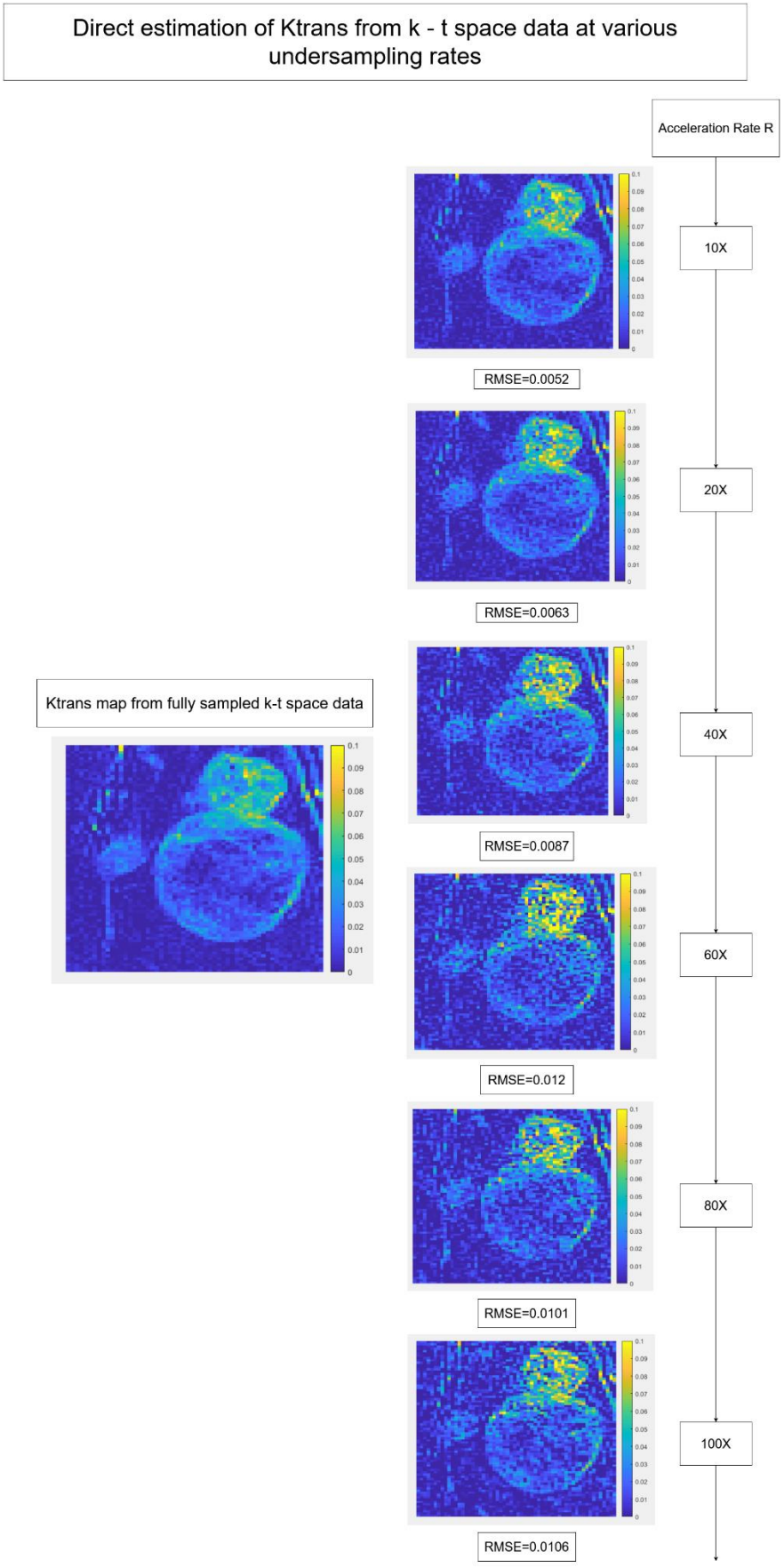

Fig 6 Direct Estimation of Ktrans from k-t space for various acceleration rates R for Dataset 1

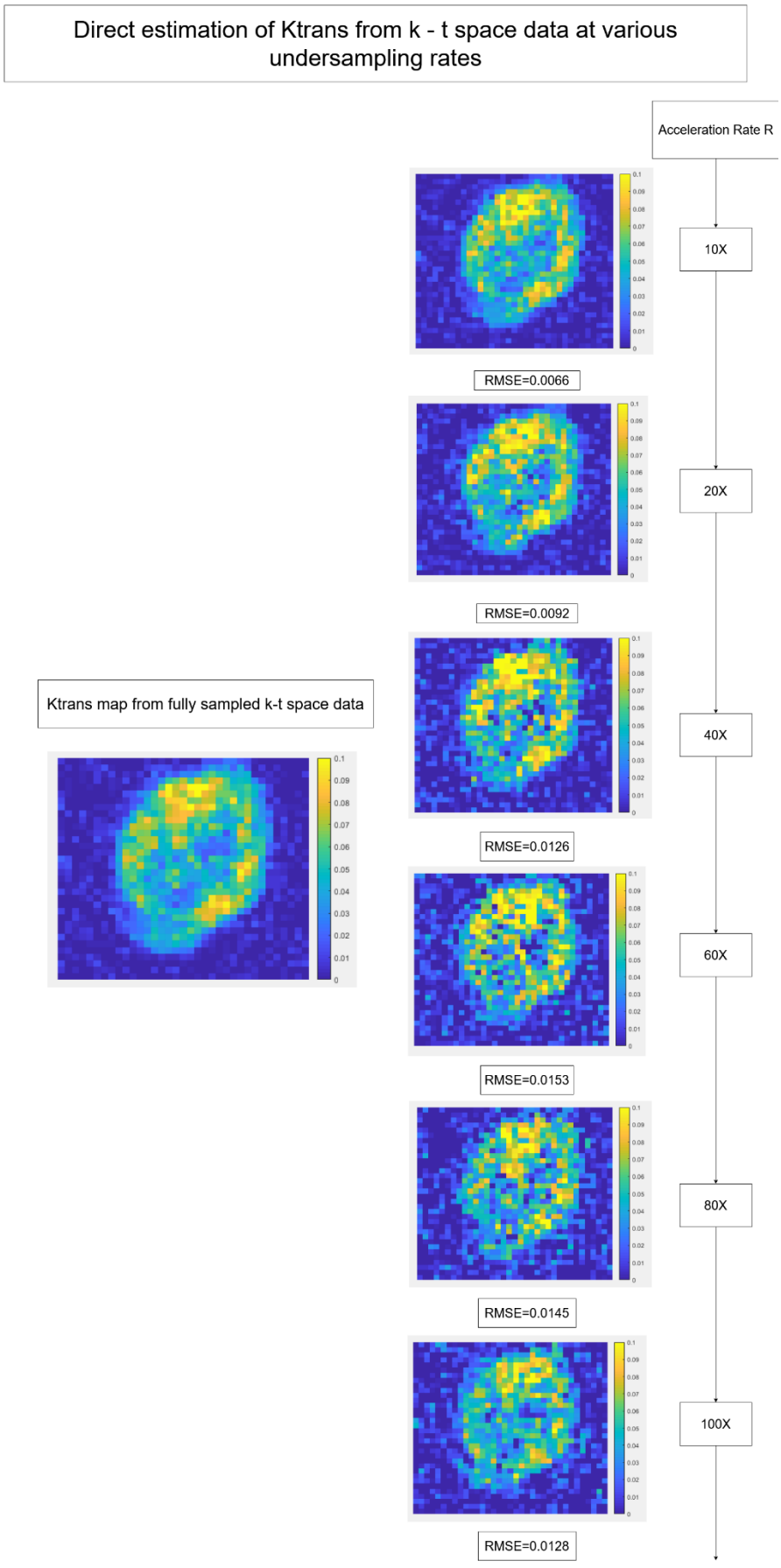

Fig 7 Direct Estimation of Ktrans from k-t space for various acceleration rates R for Dataset 2

Satisfactory reconstruction of Ktrans was achieved for both the datasets as shown by Table 2, Fig (8) and Fig (9). Ktrans maps of Dataset 1 obtained from fully sampled data and data undersampled at a rate of R=20 was compared in Fig (10). The Ktrans map obtained from the undersampled data shows a very good resemblance to the fully sampled map.

Table 2 Ktrans RMSE for Dataset 1 and Dataset 2 in the tumour region

Acceleration Rate / Dataset	Dataset 1	Dataset 2
10	0.0052	0.0066
20	0.0063	0.0092
40	0.0087	0.0126
60	0.012	0.0153
80	0.0101	0.0145
100	0.0106	0.0128

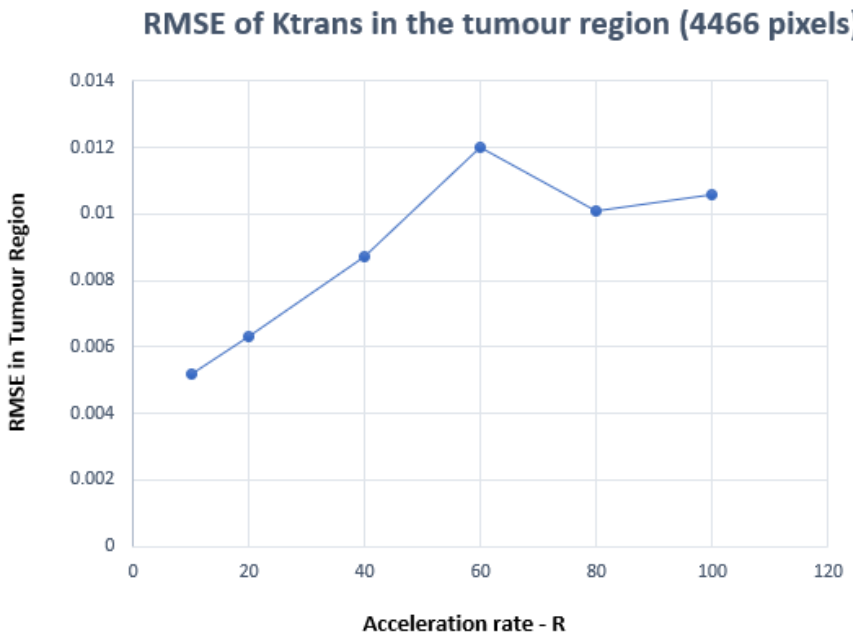

Fig 8 Ktrans RMSE in the tumour region computed for various acceleration rates for Dataset 1

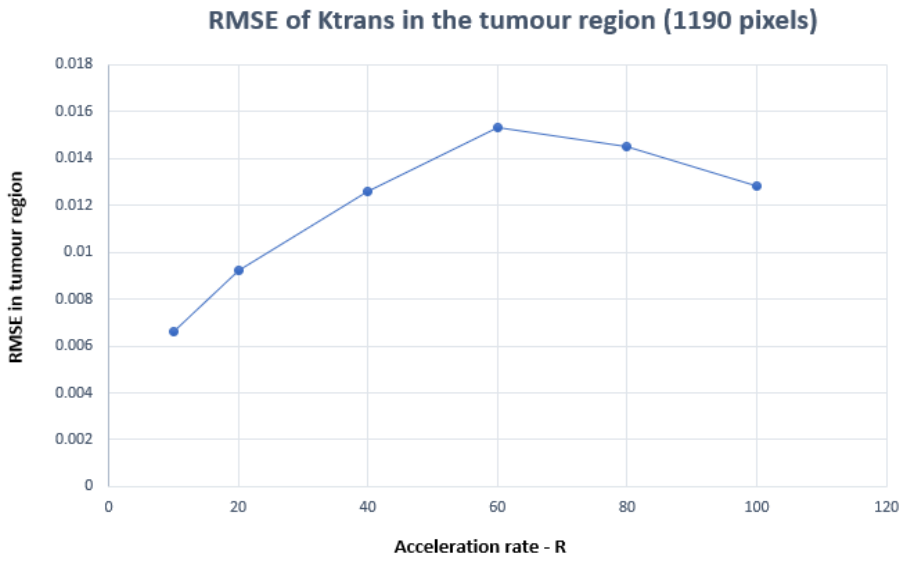

Fig 9 Ktrans RMSE in the tumour region computed for various acceleration rates for Dataset 2

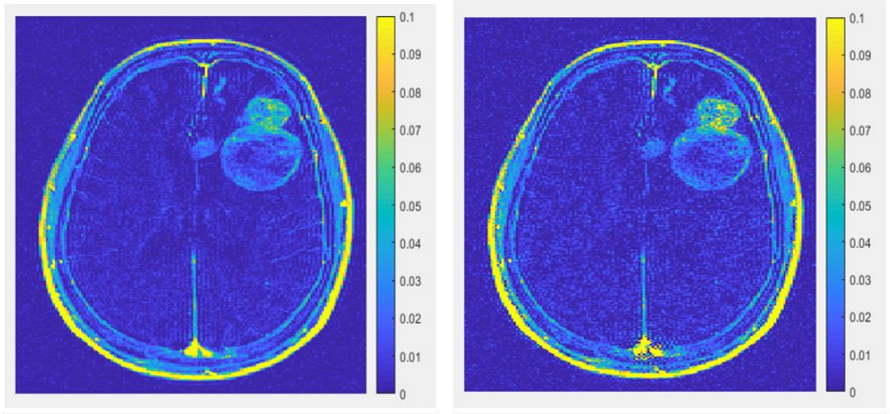

Fig 10 Comparison of Ktrans Map obtained from fully sampled k-t space data (Left) and undersampled k-t space data (Right). The Ktrans RMSE value was computed with respect to the Ktrans map obtained from the fully sampled k-t space data shown on the left.

For the proposed algorithms, all the TK parameters could be initialized to zero or Ktrans and Vp could be set to the values of Ktrans and Vp obtained through Patlak model using the undersampled data. Both the algorithms were unaffected by initialization for the two datasets, indicating that they are robust to local minima. Fig (11) compares the Ktrans estimated by the two algorithms mentioned for R=20. Cyclic optimization of TK parameters yielded erroneous results when compared to optimization of all TK parameters at the same time. Therefore, for both the datasets, the TK parameters were optimized at the same time i.e., the algorithm mentioned in eqn (9) was followed.

In order to obtain better results, Total Variation regularization was employed for Dataset 2. Fig (12) shows the Ktrans RMSE obtained in the tumour region for various undersampling rates with and without TV regularization. Estimation of Ktrans with TV regularization resulted in lower Ktrans RMSE across various undersampling rates as shown by Table 3.

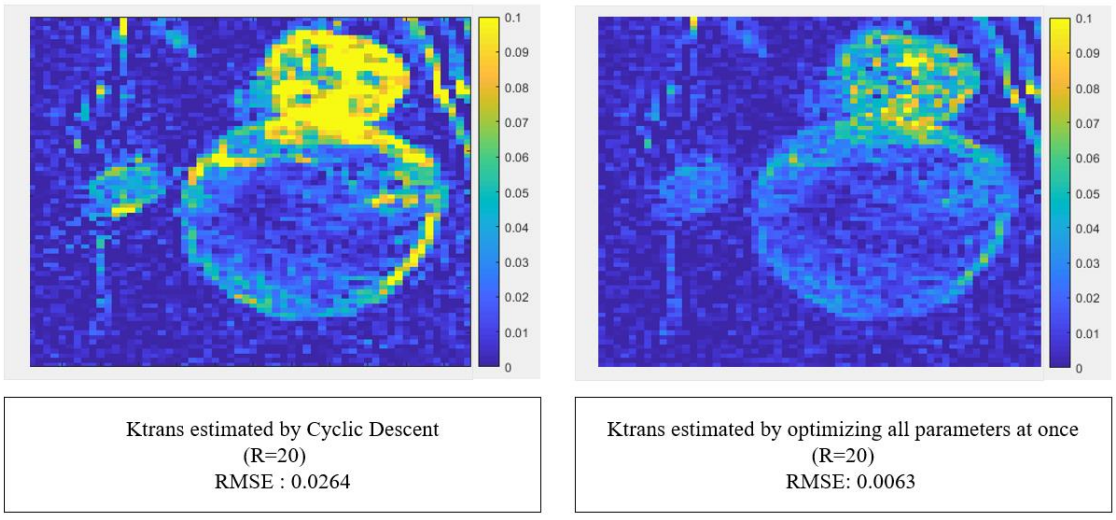

Fig 11 Comparison of the results from the two proposed algorithms for R=20. RMSE values were computed with respect to the Ktrans map of the tumour region from the fully sampled k-t space data shown in Fig (6).

Table 3 Ktrans RMSE in tumour region for Dataset 2 with and without TV Regularization

Acceleration Rate/ Dataset	Dataset 2 without TV Regularization	Dataset 2 with TV Regularization
10	0.0066	0.0062
20	0.0092	0.008
40	0.0126	0.01
60	0.0153	0.012
80	0.0145	0.0097
100	0.0128	0.0103

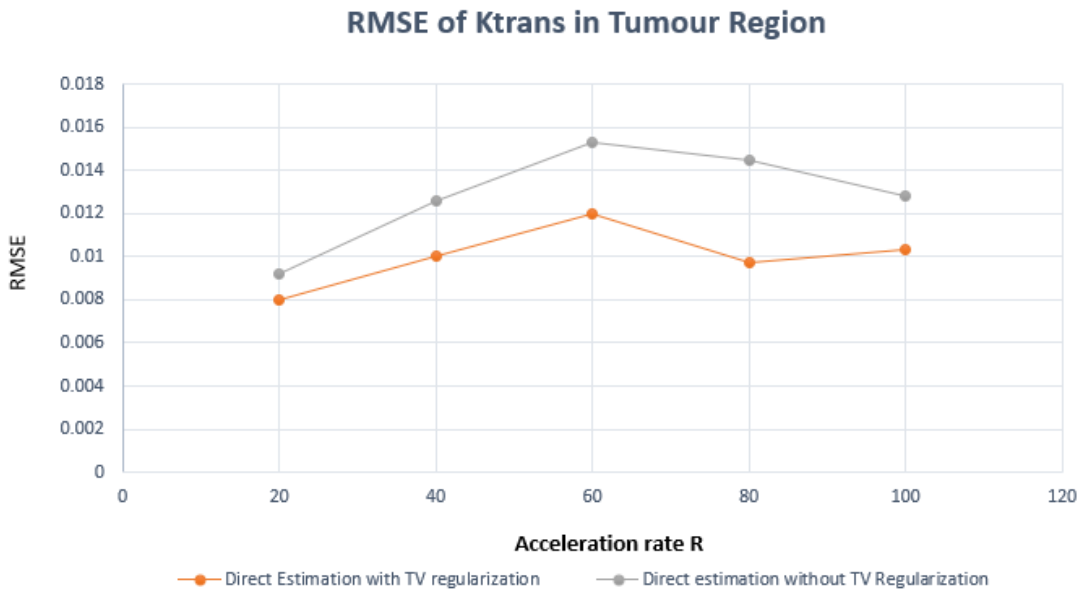

Fig 12 Comparison of Ktrans RMSE in tumour region for various acceleration rates (R) obtained with and without TV regularization for Dataset 2

5 CONCLUSION

Two algorithms for direct estimation of Ktrans using Etofts model from undersampled k-t space data were implemented with acceleration rate R ranging from 10x to 100x. The first algorithm solved a model-based minimization problem by optimizing the TK parameters at once while the latter solved the minimization problem by optimizing the TK parameters one after the other. Both the algorithms were unaffected by initialization and were robust to local minima. However, the former provided more accurate results. Satisfactory reconstruction of Ktrans map was obtained with the low RMSE values for various acceleration rates as shown in Table (2). TV regularization was also explored for suppressing noise and obtaining better results. Ktrans RMSE was compared in the tumour region, for direct estimation with and without TV regularization for Dataset 2 (in Table 3) and it was found that lower RMSE was obtained when TV regularization was enforced.

While the datasets used in this work were undersampled up to 100x, they were retrospectively sampled. This technique needs to be tested on prospectively undersampled k-t space data to obtain better insight into its efficacy. In the future, this method can be extended to more complex models such as two chamber exchange model in order to accommodate other tissue structures. A GUI that facilitates easy implementation of this technique can also be developed and made open source.

References

1. Peter Carmeliet, Rakesh K. Jain, 2000, Angiogenesis in cancer and other diseases, Nature, vol. 407, no. 6801, pp. 249-257

2. Bergers, Gabriele and Benjamin, Laura E. (2003). Tumorigenesis and the angiogenic switch. 3,

3. Guo, Yi and Lingala, Sajan Goud and Zhu, Yinghua and Lebel, R. Marc and Nayak, Krishna S. (2016). Direct estimation of tracer-kinetic parameter maps from highly undersampled brain dynamic contrast enhanced MRI. 78,

4. Klaas P. Pruessmann, Markus Weiger, Markus B. Scheidegger, Peter Boesiger, 1999, SENSE: Sensitivity encoding for fast MRI, Magnetic Resonance in Medicine, vol. 42, no. 5, pp. 952-962

5. Griswold, Mark A. and Jakob, Peter M. and Heidemann, Robin M. and Nittka, Mathias and Jellus, Vladimir and Wang, Jianmin and Kiefer, Berthold and Haase, Axel (2002). Generalized autocalibrating partially parallel acquisitions (GRAPPA). 47,

6. Lustig, Michael and Donoho, David and Pauly, John M. (2007). Sparse MRI: The application of compressed sensing for rapid MR imaging. 58,

7. Tofts, Paul S. and Brix, Gunnar and Buckley, David L. and Evelhoch, Jeffrey L. and Henderson, Elizabeth and Knopp, Michael V. and Larsson, Henrik B.W. and Lee, Ting-Yim and Mayr, Nina A. and Parker, Geoffrey J.M. and et al. (1999). Estimating kinetic parameters from dynamic contrast-enhanced t1-weighted MRI of a diffusable tracer: Standardized quantities and symbols. 10,

8. Guo, Yi and Lingala, Sajan Goud and Bliesener, Yannick and Lebel, R. Marc and Zhu, Yinghua and Nayak, Krishna S. (2017). Joint arterial input function and tracer kinetic parameter estimation from undersampled dynamic contrast-enhanced MRI using a model consistency constraint. 79,

9. Felsted, Ben K. and Whitaker, Ross T. and Schabel, Matthias and DiBella, Edward V. R. (2009). Model-based reconstruction for undersampled dynamic contrast-enhanced MRI.

10. Dikaios, Nikolaos and Arridge, Simon and Hamy, Valentin and Punwani, Shonit and Atkinson, David (2014). Direct parametric reconstruction from undersampled (k, t)-space data in dynamic contrast enhanced MRI. 18,

11. M. Schmidt. (2005). minFunc: unconstrained differentiable multivariate optimization in Matlab

12. MATLAB,2018. version 9.5.0 (R2018b), Natick, Massachusetts: The MathWorks Inc.